Mössbauer study of antiferromagnetic $CuFeS_{2-x}Se_x$

Hang Nam Ok, Kyung Seon Baek, and Eun Jung Choi
Department of Physics, Yonsei University, Seoul 120-749, Korea
(Received 16 May 1994)

$CuFeS_{2-x}Se_x$ has been studied by Mössbauer spectroscopy and x-ray diffraction. The crystal is found to have a tetragonal structure and the lattice constants a_0 and c_0 increase linearly with increasing selenium concentration. It is noteworthy that the replacement of S by Se in the chalcopyrite decreases the strength of both the superexchange interaction and the interatomic binding. As the interatomic distance increases by 1%, the magnetic hyperfine field and the Debye temperature decrease by 0.8 and 6%, respectively. The iron ions are found to be in ferric states.

The chalcopyrite $CuFeS_2$ is known to have a tetragonal structure.[1] Its lattice constants[2] are reported to be $a_0=5.289$ Å and $c_0=10.423$ Å. Its metallic atoms have almost perfect tetrahedral coordination with four neighboring sulfur ions. According to neutron diffraction,[3] magnetic susceptibility and torque measurements,[4] chalcopyrite is antiferromagnetic below about 550 °C and the spin direction is [001].

Piekoszewski, Suwalski, and Ligenza[5] observed a six-line Mössbauer pattern of a natural chalcopyrite sample from Banska Stiavnica from 80 to 700 K. They found progressive decomposition of their chalcopyrite sample above 600 K and the Mössbauer spectra of partly decomposed samples exhibited Zeeman splitting in combination with a central peak.

In an attempt to study the effects of interatomic separation on the magnetic properties and interatomic binding, we prepared $CuFeS_{2-x}Se_x$ samples. Since both sulfur and selenium ions have the same electron configurations outside completely filled shells, a comparative study of $CuFeS_2$ and $CuFeS_{2-x}Se_x$ would reveal these effects of interatomic separation.

Synthesis of the $CuFeS_{2-x}Se_x$ ($x=0.0,0.2,0.4,0.6$) samples was accomplished by the following direct-composition method. Iron powder of 99.9995% purity and copper powder of 99.999% purity were reduced by hydrogen gas at 750 °C. A mixture of the proper proportions of these powders, sulfur of 99.9999% purity, and selenium of 99.999% purity was sealed into an evacuated quartz tube which had been previously heated to 750 °C in a hydrogen atmosphere to eliminate oxygen adsorbed into the quartz wall. The sealed mixture was heated at 950 °C for 120 h, and then slowly cooled down to room temperature at a rate of 10 °C/h. The product was reground, refired at 950 °C for 120 h, and then cooled down to room temperature. The sample was ^{57}Fe enriched to 5 at. % of the metal atoms in the samples for Mössbauer measurements.

X-ray diffraction patterns of the samples were obtained with Cu $K\alpha$ radiation. A slow scanning speed of 0.25° advance in 2θ per min was used in order to optimize resolution of the closely spaced reflections. A Mössbauer spectrometer of the electromechanical type was used in the constant-acceleration mode. A ^{57}Co single-line source in a rhodium matrix was used at room temperature. To produce a uniform thickness over the area of the Mössbauer absorber, each sample was mixed with boron nitride powder and clamped between two thin boron nitride plates.

The x-ray diffraction patterns showed that all the samples of $CuFeS_{2-x}Se_x$ ($0\le x\le 0.6$) had a tetragonal structure. Close examination and analysis of the observed peak positions and intensities show that the samples have the same tetragonal structure as that found by Pauling and Brockway.[1] Figure 1 shows the calculated lattice constants a_0 and c_0, which increase linearly with increasing selenium concentration x. This can be expected in view of the fact that the ionic radius of 1.98 Å for Se^{2-} ions is larger than the 1.84 Å for S^{2-} ions.[6]

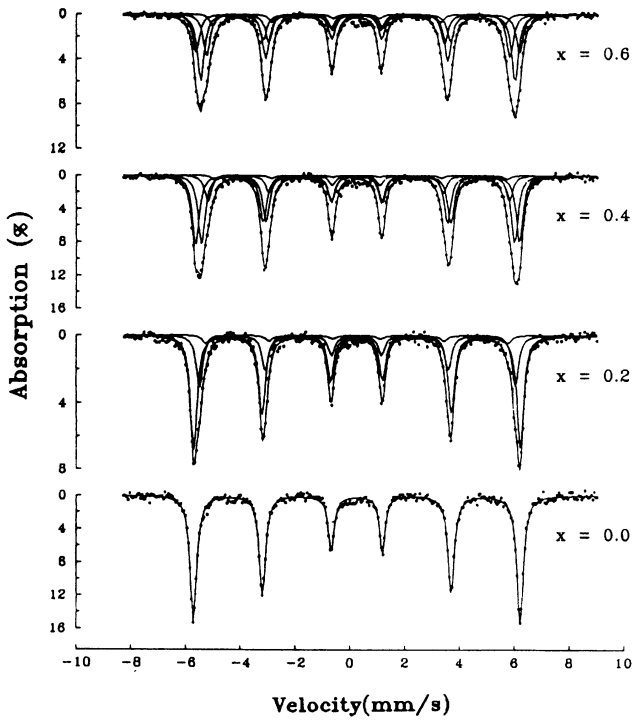

FIG. 1. Variation of the lattice constants a_0 and c_0 of the tetragonal structure with composition for $CuFeS_{2-x}Se_x$.

 ©1994 The American Physical Society

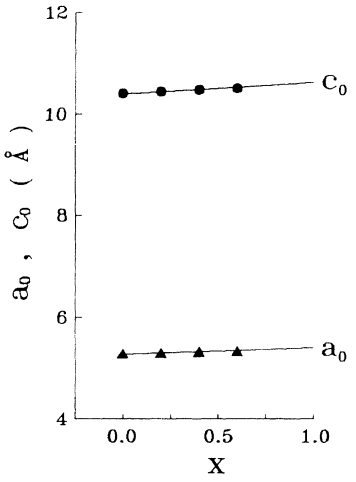

FIG. 2. Mössbauer spectra of $CuFeS_{2-x}Se_x$ samples ($x=0.0,0.2,0.4,0.6$) at 50 K. The solid lines through the data points are least-squares fits of one, three, or four sets of six-line (Lorentzian) patterns to the experimental data. The solid lines above the data points are the individual component lines.

Mössbauer spectra of $CuFeS_{2-x}Se_x$ were measured at various absorber temperatures ranging from 4 up to 400 K, which was arbitrarily chosen to be a safe upper limit of temperature in view of decomposition observed above 600 K. Figure 2 shows Mössbauer spectra at 50 K for the $CuFeS_{2-x}Se_x$ ($x=0.0,0.2,0.4,0.6$) samples. The Mössbauer spectra for the $CuFeS_2$ consist of resonant absorption lines with narrow linewidths. On the other hand, the Mössbauer spectra for $CuFeS_{2-x}Se_x$ ($x=0.2,0.4,0.6$) are composed of broad six-line hyperfine patterns. The broadening of the spectra is interpreted as being due to a distribution of hyperfine fields at the Fe site caused principally by a random distribution of the nearest-neighbor sulfur or selenium ions. The relative intensity of the Fe site with n selenium nearest neighbors is given by

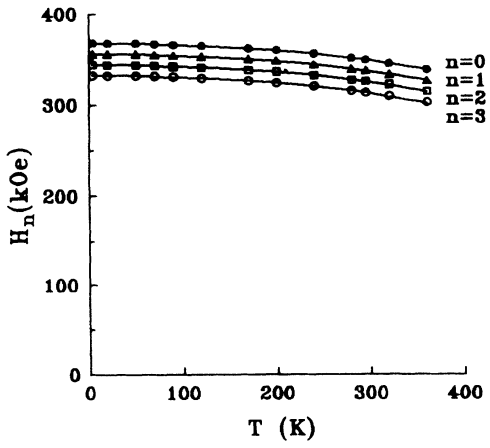

FIG. 3. Temperature dependence of the magnetic hyperfine fields at iron sites with n selenium nearest neighbors in the $CuFeS_{1.4}Se_{0.6}$ sample.

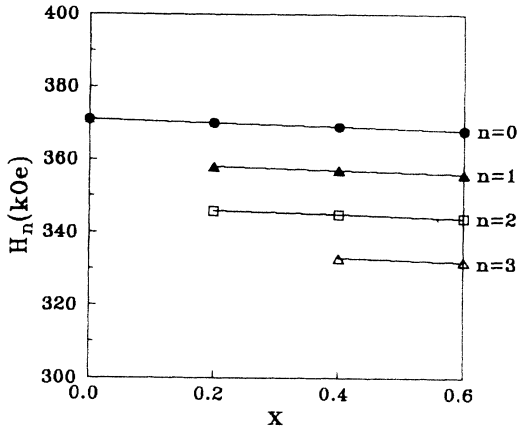

FIG. 4. Magnetic hyperfine fields at 4 K for the iron sites with n selenium nearest neighbors in the $CuFeS_{2-x}Se_x$ samples ($x=0.0,0.2,0.4,0.6$).

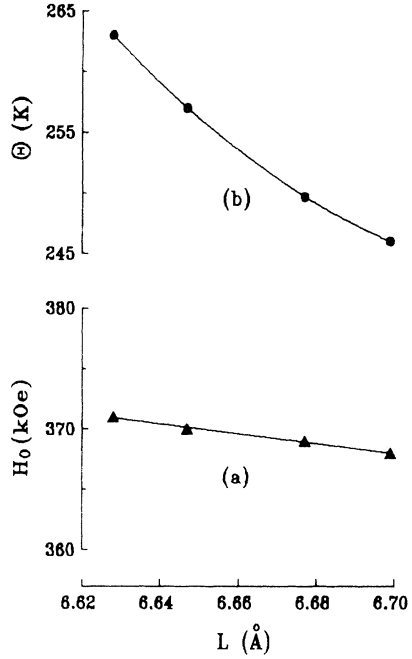

FIG. 5. (a) Magnetic hyperfine fields H_0 for iron sites with four sulfur nearest neighbors at 4 K in the $CuFeS_{2-x}Se_x$ samples vs a linear dimension L, defined by $L=(a_0^2c_0)^{1/3}$. (b) Debye temperature of the $CuFeS_{2-x}Se_x$ samples vs L.

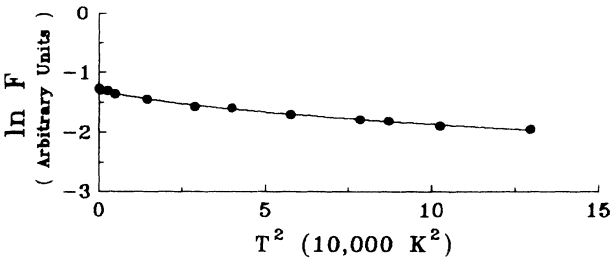

FIG. 6. Natural logarithm of the resonant absorption area F vs T^2 for $CuFeS_{1.4}Se_{0.6}$.

TABLE I. Probability $P(n,x)$ of an iron atom having n selenium nearest-neighbor ions in the $CuFeS_{2-x}Se_x$ sample.

x/n	0	1	2	3	4
0.0	1.0000	0.0000	0.0000	0.0000	0.0000
0.2	0.6561	0.2916	0.0486	0.0036	0.0001
0.4	0.4096	0.4096	0.1536	0.0256	0.0016
0.6	0.2401	0.4116	0.2646	0.0756	0.0081

$$p(n,x)=\left[\frac{4}{n}\right]\left[\frac{x}{2}\right]^n\left[\frac{2-x}{2}\right]^{4-n}, \quad (1)$$

where $x/2$ represents the number of selenium ions per anion site in the $CuFeS_{2-x}Se_x$ sample. The calculated values of $P(n,x)$ are shown in Table I.

Using a least-squares computer program, one, three, or four sets of six Lorentzian lines were fitted to the Mössbauer spectra for $x=0,0.2,0.4$, and 0.6 under the usual constraints,[7] which are valid when the quadrupole interaction is much weaker than the magnetic hyperfine interaction. The magnetic hyperfine fields for the locally different iron sites are assumed to obey the following relationship:[8]

$$H_n=H_0-n\Delta H , \quad (2)$$

where n is the number of selenium ions among the four nearest-neighboring anion sites of the iron ion that has a magnetic hyperfine field H_n. H_0 is the hyperfine field at an iron ion that has no selenium nearest neighbors. ΔH is the decrement in the hyperfine field as a result of replacing a sulfur ion by a selenium ion.

The isomer-shift values at room temperature range from 0.32 ($x=0$) to 0.36 mm/s ($x=0.6$) relative to the iron metal value, indicating that the iron ions are ferric.[9] This assignment of the charge state is consistent with the magnitudes of the magnetic hyperfine fields as shown in Figs. 3 and 4.

Since ferric ions have neither orbital nor dipolar contributions[10] to the magnetic hyperfine field, the magnetic hyperfine field in our samples is proportional to the ferric-ion spin aligned by the superexchange interactions. It is noted in Fig. 4 that the magnetic hyperfine field H_n decreases linearly with increasing selenium concentration x. This implies that the increase of the interatomic separation decreases the magnetic hyperfine field or weakens the superexchange interaction, because the lattice constants a_0 and c_0 or the interatomic separation increase linearly with increasing selenium concentration, as shown in Fig. 1. Figure 5(a) shows H_0 at 4 K as a function of a linear dimension L defined by

$$L=(a_0^2c_0)^{1/3} , \quad (3)$$

the percentage increase of which may represent that of the interatomic separation. Figure 5(a) indicates that H_0 decreases by 0.8% per 1% increase of interatomic separation.

TABLE II. Quadrupole shift ΔE_Q at iron sites with n selenium nearest neighbors in the $CuFeS_{2-x}Se_x$ samples ($x=0.0,0.2,0.4,0.6$) at all temperatures ranging from 4 to 400 K. The number in parentheses indicates estimated error in the last digit.

n	0	1	2	3
ΔE_Q (mm/s)	0.00(1)	0.02(1)	0.03(1)	0.03(1)

It is also noted in Figs. 3 and 4 that the magnetic hyperfine fields decrease monotonically with increasing number of selenium nearest neighbors; at 4 K, H_n decreases by $\Delta H=12$ kOe whenever a sulfur nearest neighbor of Fe is replaced by a selenium ion. The implication of this is that the superexchange interaction for the Fe^{3+}-Se-Fe^{3+} link is weaker than that for the Fe^{3+}-S-Fe^{3+} link.

Table II lists the quadrupole shifts defined by $\Delta E_Q=(V_6-V_5+V_1-V_2)/4$, where V_i represents the position of the ith absorption line. It can be seen in Table II that the quadrupole shifts for the iron site ($n=0$) surrounded only by sulfur ions vanish in consistence with the almost perfect tetrahedral coordinations for the site. It is also noted in Table II that the quadrupole shift increases slightly with increasing number of selenium nearest neighbors, reflecting symmetry breaking due to selenium ions.

Figure 6 shows $\ln F$ versus T^2 for $CuFeS_{1.4}Se_{0.6}$, where F stands for the total resonant absorption area of a Mössbauer spectrum at T. F is proportional to the recoil-free fraction f. The Debye model gives the following expression[11] for the recoil-free fraction:

$$f=\exp\left[-\frac{3E_R}{2k_B\Theta}\left[1+\frac{4T^2}{\Theta^2}\int_0^{\Theta/T}\frac{x\,dx}{e^x-1}\right]\right], \quad (4)$$

where E_R is the recoil energy of ^{57}Fe for the 14.4-keV γ ray. Θ and k_B represent the Debye temperature and Boltzmann constant, respectively. The Debye temperature can be calculated from the temperature dependence of the resonant absorption area of each subspectrum at low temperatures. The calculated results for the $CuFeS_{2-x}Se_x$ samples ($x=0.0,0.2,0.4,0.6$) are shown in Fig. 5(b). It is noted in this figure that the Debye temperature decreases approximately exponentially with increasing linear dimension L of the unit cell. This implies that the increase of the interatomic separation decreases interatomic binding. For 1% increase of interatomic separation, the Debye temperature decreases by 6%.

The present studies were supported by the Basic Science Research Institute Program, the Ministry of Education, 1994, Project No. 2424 and by Yonsei University, Project No. 93-106.

[1]L. Pauling and L. O. Brockway, Z. Kristallogr. **82**, 188 (1932).
[2]S. R. Hall and J. M. Stewart, Acta Crystallogr. Sec. B **29**, 579 (1973).
[3]G. Donnay, L. M. Corliss, J. D. H. Donnay, N. Elliot, and J. M. Hastings, Phys. Rev. **112**, 1917 (1958).
[4]T. Teranishi, J. Phys. Soc. Jpn. **16**, 1881 (1961).
[5]J. Piekoszewski, J. Suwalski, and. S. Ligenza, Phys. Status Solidi **29**, K99 (1968).

[6]C. Kittel, *Introduction to Solid State Physics* (Wiley, New York, 1986), p. 76.

[7]K. S. Baek, E. J. Hahn, and H. N. Ok, Phys. Rev. B **36**, 763 (1987).

[8]W. E. Sauer and R. J. Reynik, in *Mössbauer Effect Methodology,* edited by I. G. Gruverman (Plenum, New York, 1968), Vol. IV, p. 201; M. B. Stearns, Phys. Rev. **147**, 439 (1966).

[9]M. R. Spender, J. M. D. Coey, and A. H. Morrish, Can. J. Phys. **50**, 2313 (1972); H. N. Ok, Y. Chung, and J. G. Kim, Phys. Rev. B **20**, 4550 (1979).

[10]F. K. Lotgering, R. P. van Stapele, G. H. A. M. van der Steen, and J. S. van Wieringen, J. Phys. Chem. Solids **30**, 799 (1969).

[11]R. L. Mössbauer and W. H. Wiedermann, Z. Phys. **159**, 33 (1960); B. Kaufmann and H. J. Lipkin, Ann. Phys. (N.Y.) **18**, 294 (1962).